

PenTiDef: Enhancing Privacy and Robustness in Decentralized Federated Intrusion Detection Systems against Poisoning Attacks

Phan The Duy^{1,2,3}, Nghi Hoang Khoa^{1,2,3}, Nguyen Tran Anh
Quan^{1,2,3}, Luong Ha Tien^{1,2,3}, Ngo Duc Hoang Son^{1,2,3},
Van-Hau Pham^{1,2,3*}

¹Information Security Lab, University of Information Technology, Ho
Chi Minh City, Vietnam.

²Vietnam National University, Ho Chi Minh City, Vietnam.

³VNU-HCM Information Security Center, Ho Chi Minh City, Vietnam.

*Corresponding author(s). E-mail(s): haupv@uit.edu.vn;

Contributing authors: duypt@uit.edu.vn; khoanh@uit.edu.vn;
20521793@gm.uit.edu.vn; 20520802@gm.uit.edu.vn; sonndh@uit.edu.vn;

Abstract

Context: The increasing deployment of Federated Learning (FL) in Intrusion Detection Systems (IDS) introduces new challenges related to data privacy, centralized coordination, and susceptibility to poisoning attacks. While significant research has focused on protecting traditional FL-IDS with centralized aggregation servers, there remains a notable gap in addressing the unique challenges of decentralized FL-IDS (DFL-IDS).

Objectives: This study aims to address the limitations of traditional centralized FL-IDS by proposing a novel defense framework tailored for the decentralized FL-IDS architecture, with a focus on privacy preservation and robustness against poisoning attacks.

Methods: We propose *PenTiDef*, a privacy-preserving and robust defense framework for DFL-IDS, which incorporates Distributed Differential Privacy (DDP) to protect data confidentiality and utilizes latent space representations (LSR) derived from neural networks to detect malicious updates in the decentralized model aggregation context. To eliminate single points of failure and enhance trust without a centralized aggregation server, *PenTiDef* employs a blockchain-based decentralized coordination mechanism that manages model aggregation, tracks update history, and supports trust enforcement through smart contracts.

Results: Experimental results on CIC-IDS2018 and Edge-IIoTSet demonstrate that PenTiDef consistently outperforms existing defenses (e.g., FLARE, FedCC) across various attack scenarios and data distributions.

Conclusion: These findings highlight the potential of PenTiDef as a scalable and secure framework for deploying DFL-based IDS in adversarial environments. By leveraging privacy protection, malicious behavior detection in hidden data, and working without a central server, it provides a useful security solution against real-world attacks from untrust participants.

Keywords: Intrusion Detection System, Decentralized Federated Learning, Blockchain, Privacy, Poisoning Attacks

1 Introduction

In the current era, the increasing prevalence of the Internet has increased the risk of unauthorized intrusions, prompting organizations to improve systems to check vulnerabilities in critical information systems. Intrusion Detection Systems (IDS) are effective tools for detecting network attacks by monitoring traffic and identifying abnormal behaviors. In the booming of Artificial Intelligence (AI), the Machine Learning (ML) advancements have led to its application in IDS, aiming for breakthroughs in information security. However, ML-based IDS require extensive training data from various sources, including multiple attack types, but data sharing is limited due to privacy concerns. In this context, Federated Learning (FL) has emerged as a potential solution to balance data training performance with data security and privacy [1] [2]. This method does not require explicit sharing of training data, as traditional Centralized Federated Learning (CFL) methods do.

Although FL is promising, it has drawbacks when faced with unethical actors. Attackers can perform poisoning attacks by uploading incorrect output parameters, degrading the model's performance, and causing training errors. Multiple malicious entities can exacerbate these issues. Thus, combining blockchain with FL to collaboratively detect fraud is a compelling research area aimed at enhancing the security and reliability of anti-fraud systems.

Recent studies [3] [4] on the application of blockchain to create a decentralized, tamper-proof database have shown significant potential to improve information system security and reliability. Blockchain ensures that all transactions and data changes are recorded immutably and transparently, preventing tampering and fraud. Its decentralized nature eliminates single points of failure, increasing the resilience and availability of the system. This combination protects data from attacks and fosters a trust environment in which participants can independently verify and audit transactions.

Although FL enables collaborative model training without exchanging private information, it still poses privacy risks. Research shows that sensitive information can be leaked through gradient exchanges. Attackers can deduce private details such as class representations, membership, and attributes from gradients, and in severe

cases, reassemble original training samples without prior knowledge of the data. Gradients, calculated using private training data through backpropagation, are vulnerable to breaches. Thus, protecting privacy in FL is crucial, requiring robust safeguards to prevent illegal access through gradient-based attacks.

Several studies [5] [6] have proposed methods to preserve privacy during FL training. Homomorphic Encryption (HE) allows arithmetic operations on encrypted data, preserving model performance, but requiring substantial memory and processing time, leading to high costs. Secure Multi-Party Computation (SMPC) [7] [8], like SecureML [9], enables joint computations without revealing private data, but also incurs high costs and requires simultaneous coordination of all parties. Therefore, to save costs and enhance the scalability of the Decentralized Federated Learning (DFL) model, we chose to apply the Differential Privacy (DP) method. DP was initially designed for single-database scenarios, where the database server responds to queries by adding controlled randomness to ensure privacy. Compared to encryption-based methods, DP balances privacy and accuracy by adding noise to the data to ensure computational efficiency, prevent attackers from recovering or inferring the original data, and not severely impact the utility of the data.

Besides privacy concerns, another significant barrier to DFL adoption is its vulnerability to poisoning attacks [5]. Malicious participants can degrade model performance through data poisoning or model poisoning, leading to untargeted attacks that reduce overall performance or targeted attacks that create specific biases. These varied strategies make it challenging to identify and prevent attacks, necessitating robust protective measures and thorough monitoring.

Most defense mechanisms rely on anomaly detection [10] [11] [12] to eliminate abnormal models. However, these methods face significant computational burdens and difficulties in detecting malicious models due to the large number of parameters in machine learning architectures. This hampers scalability in DFL environments. Moreover, some methods require knowing the number of malicious agents in advance, which is impractical. Additionally, distinguishing between malicious and benign model parameters, especially with non-IID data, remains challenging [13] [14].

Consequently, robust aggregation methods [15] [16] [17] have emerged. Among them, a novel approach uses the latent space, such as FedCC [18], FLARE [19], and Fed-LSAE [20]. These modules extract Penultimate Layer Representations (PLR) and perform comparisons between models. These methods have shown that the PLR of benign model parameters follow a similar pattern, while malicious PLR diverge in different directions. However, the FLARE [19] module requires an auxiliary dataset to calculate PLR, which violates the privacy rules for the collaborating entities mentioned earlier. In contrast, the FedCC [18] method extracts the PLR directly from the updated models without using an auxiliary dataset, which may cause instability in the PLR if each local model is trained in a different data distribution. To overcome these weaknesses, the Fed-LSAE [20] model inputs the PLR of each local model into an AutoEncoder (AE) with the goal of minimizing PLR instability and extracting the LS representation of PLR through the bottleneck layer, thereby reducing the parameter size assuming the PLR is still considerable.

Inspired by their previous methods, in this paper, we propose the PenTiDef framework - (Pen)ultimate layer representation approach for (T)rust and pr(i)vacu preserving (De)centralized (F)ederated IDS. Our framework addresses key challenges in applying FL to intrusion detection systems (IDS), including centralized aggregation risks, privacy leakage through gradients, and vulnerability to poisoning attacks under non-IID conditions. In summary, the main contribution of this paper are as follows:

- A decentralized FL architecture for IDS that eliminates the dependency on a central server by leveraging blockchain-based coordination. This improves fault tolerance, transparency, and trust among collaborating nodes through smart-contract-enforced interaction.
- A privacy-preserving defense mechanism based on Distributed Differential Privacy (DDP), which introduces randomized noise at the local level without degrading model performance, addressing the privacy risks of gradient leakage in FL.
- A latent space-based anomaly detection strategy that combines AutoEncoder (AE)-compressed penultimate layer representations with Centered Kernel Alignment (CKA) and unsupervised clustering to identify poisoned updates, even under non-IID data distributions.
- A lightweight and scalable integration of defense and coordination mechanisms that avoids the need for auxiliary datasets, prior knowledge of adversaries, or synchronized model training, thus improving robustness and training efficiency in heterogeneous environments.
- Comprehensive experimental validation on benchmark data sets (CIC-IDS2018 and Edge-IIoTSet), demonstrating superior detection performance and system scalability compared to state-of-the-art defenses (e.g., FLARE, FedCC) in various attack scenarios and network conditions.

This article is organized as follows in the remaining sections. In Section 2, relevant papers on privacy attacks and poisoning attacks against FL-based models, and their defenses are discussed. The threat model is presented in Section 3 to determine the assumption about attackers in our works. Section 4 then discusses the approach and threat model. Next, in Section 5, we outline the research questions and experimental scenarios to benchmark the framework. The experimental setups, dataset and evaluation metrics are presented in Section 6. Following that, Section 7 provides the experimental results and analysis of the PenTiDef performance. The discussion on achievement and limitation of our work is mentioned in Section 8. In Section 9, we finally conclude the paper.

2 Related work

2.1 Privacy Attacks in the Context of FL

Although FL avoids direct sharing of raw data among participants, it remains susceptible to privacy leakage through exchanged model updates. Prior studies [21–23] have demonstrated that gradients and consecutive model snapshots can inadvertently expose sensitive information about local training data. This vulnerability stems from

Table 1: Comparison between DP categorizations

DP type	Trusted aggregator	Adding noise by	Privacy Guarantee
CDP	Yes	Aggregator	Aggregated value
LDP	No	User	Locally released value
DDP	No	User	Aggregated value

the fact that deep learning models often encode latent representations beyond the primary task objective.

Adversaries can exploit these gradients to perform various inference attacks, aiming to recover private information such as class representatives, membership status, sample attributes, and even training inputs or labels. One notable example is the GAN-based attack, where malicious clients leverage Generative Adversarial Networks to synthesize prototypical data from other participants. Another common threat is membership inference, which seeks to determine whether a specific data point was part of a client’s training set. These attacks can be executed passively—by observing model updates—or actively, through deliberate manipulation of the training process to amplify information leakage [5].

These findings underscore the importance of incorporating robust gradient protection mechanisms in FL, especially in privacy-sensitive applications such as healthcare, finance, and smart environments.

2.2 Defense Mechanisms Against Privacy Attacks in FL

Preserving privacy in FL poses distinct challenges due to decentralized data, statistical heterogeneity, and limited communication reliability. Among the major privacy-preserving strategies proposed, three prominent approaches are Homomorphic Encryption (HE), Secure Multi-Party Computation (SMPC), and Differential Privacy (DP) [5, 27].

HE enables computations on encrypted data without decryption and is categorized into Fully, Somewhat, and Partially Homomorphic Encryption. While Fully HE supports arbitrary computations, it is computationally intensive and impractical for real-time FL scenarios. In contrast, Partially HE schemes—such as RSA, El Gamal, and Paillier—are more efficient but limited in function [5]. Despite its theoretical appeal, HE incurs substantial memory and runtime overhead, hindering scalability in decentralized FL (DFL).

SMPC allows multiple parties to collaboratively compute functions over private inputs without revealing them. For instance, Şahinbaş and Catak [28] proposed an SMPC-based framework for FL in healthcare IoT, enabling secure model training while preserving data confidentiality. Similarly, SecureML by Mohassel and Zhang [29] enables distributed model training via secret sharing between non-colluding servers. However, both approaches suffer from high computational and communication costs, making them less suitable for large-scale or resource-constrained environments.

In contrast, DP provides a lightweight yet effective privacy mechanism by introducing calibrated noise into data or model updates. DP is commonly categorized into

three variants: Centralized DP (CDP), Local DP (LDP), and Distributed DP (DDP), as summarized in Table 1. CDP depends on a trusted aggregator to inject noise after model update collection, which introduces a central point of failure and regulatory concerns. LDP removes the need for a trusted server by having clients perturb data locally; however, it often compromises model accuracy in high-dimensional settings.

DDP overcomes the limitations of CDP and LDP by distributing noise addition across participants using stable distributions, such as Gaussian [30] and Binomial [31]. In the context of DFL, DDP enhances privacy without requiring centralized trust, reduces the impact of noise on model utility, and supports scalability. These characteristics make DDP particularly suitable for privacy-preserving learning in adversarial and heterogeneous FL environments.

Table 2: Comparison of studies on defending against poisoning attacks in FL

Work	Attack strategies	FL approach	Feature	Detection mechanism	Privacy mechanism	Non-IID	Dataset
ShieldFL [24]	+Untargeted: - Label flipping +Targeted: - Label flipping	CFL	Local model gradient	Cosine similarity	HE	×	MNIST KDDCup Amazon
FLARE [19]	+Untargeted: - Attack-Krum-Untargeted - Attack-TM-Untargeted +Targeted: - Attack-Krum-Backdoor - Attack-Coomed-Backdoor	CFL	PLR	Maximum mean discrepancy	-	-	fMNIST CIFAR-10 Kather
FedCC [18]	+Untargeted: - Untargeted-Krum - Untargeted-Med +Targeted: - Backdoor	CFL	PLR	CKA similarity with Clustering	-	-	fMNIST CIFAR10 CIFAR100
Liu et al. [25]	+Untargeted: - Model poisoning - Plaintext attack - Untargeted-Med +Targeted: - Backdoor injection - GAN	DFL	Model parameters	Low-accuracy detection in (m,n) threshold aggregated models	Secret Sharing Differential Privacy Blockchain	-	KDDCup99
DeepBlockIoTNet [26]	+Untargeted: - Model poisoning - Untargeted-Med +Targeted: - Adversarial injection - Server poisoning	DFL	Encrypted gradient, signature	Voting, Model accuracy deviation	Public-Key Encryption, Digital Signature, Blockchain	-	COCO
Fed-LSAE [20]	+Untargeted: - Label flipping - Weight scaling - Untargeted-Med +Targeted: - GAN	CFL	Computed LSR from PLR via AE	CKA similarity with Clustering of LSRs	-	×	CIC-ToN-IoT N-BaIoT
PentiDef (Our)	+Untargeted: - Label flipping - Weight scaling - Untargeted-Krum - Untargeted-Med +Targeted: - Backdoor - GAN	DFL	Computed LSR from PLR via AE	CKA similarity with Clustering of LSRs	DDP	×	Edge-IIoTSet CIC-IDS2018

2.3 Poisoning Attacks and Defense Mechanisms in FL

Despite its privacy advantages, FL remains vulnerable to poisoning attacks, which aim to degrade global model performance through manipulated client updates. These attacks are typically categorized as data poisoning—where adversaries inject mislabeled or malicious samples into their local datasets—and model poisoning, which involves directly altering model parameters to influence aggregation. Model poisoning is generally more effective, as it circumvents the need for data manipulation and directly impacts global convergence.

Recent studies have explored various attack strategies. Zhang et al. introduced GAN-based attacks [32], where adversaries use the global model as a discriminator to generate malicious samples that appear benign. Building on this, PoisonGAN [33] targets FL in edge computing by injecting adversarial updates crafted via generative models, demonstrating high success rates in both backdoor and label-flipping scenarios. Similarly, the PoisonedFL framework [34] utilizes multi-round consistency among malicious clients to evade detection, outperforming multiple state-of-the-art defenses in targeted settings.

In response, several defense mechanisms have been proposed. ShieldFL [24] employs homomorphic encryption with cosine similarity scoring and a Byzantine-tolerant aggregation strategy to mitigate poisoning risks. While effective, its cryptographic overhead limits scalability in large-scale deployments.

Recent approaches have focused on leveraging latent space representations (LSR) for model-level anomaly detection. FLARE [19] extracts penultimate-layer representations (PLR) using an auxiliary dataset to compute trust scores, filtering out low-trust models. However, its reliance on external data introduces potential privacy leakage and reduces generalizability. FedCC [18] addresses this by using the CKA algorithm to compare local and global PLRs without auxiliary data, clustering models via K-Means. Although FedCC improves resilience against model poisoning, it may suffer from PLR instability in non-IID settings.

To overcome these limitations, Fed-LSAE [20] introduces an AutoEncoder-based approach that compresses PLRs into stable LSRs without auxiliary data or prior knowledge. By distinguishing malicious from benign models based on latent characteristics, Fed-LSAE improves detection accuracy in non-IID environments and reduces the risk of false positives.

2.4 Improvement over Prior Research

While prior research has made considerable progress in defending FL systems against poisoning attacks, existing approaches still face critical limitations when applied in DFL environments. Methods such as FLARE [19] and FedCC [18] assume a centralized server for model aggregation and often depend on auxiliary datasets or predefined trust assumptions. These constraints not only compromise privacy but also hinder scalability and deployment in realistic, heterogeneous settings. Although Fed-LSAE [20] mitigates some of these concerns by avoiding external data and enhancing detection via latent representations, it remains tied to a centralized architecture and does not explicitly incorporate privacy-preserving mechanisms.

These efforts underscore the need for robust, privacy-preserving defenses that remain effective under data heterogeneity and decentralized coordination—challenges that our proposed framework, PenTiDef, is specifically designed to address. In particular, PenTiDef introduces a latent space-based defense strategy that captures penultimate-layer representations and compresses them via an AutoEncoder to produce stable latent features (LSRs) for anomaly detection. To further protect participants’ data, PenTiDef employs a DDP mechanism, which injects calibrated noise at the client level while preserving model utility. Moreover, to eliminate the reliance on a central aggregator and strengthen system transparency, PenTiDef integrates a blockchain-based coordination layer that governs model aggregation and enforces trust through smart contract-driven reward and punishment policies.

Importantly, PenTiDef is capable of detecting both targeted and untargeted poisoning attacks in the presence of non-IID data distributions—a frequent challenge in real-world deployments. By jointly addressing decentralized coordination, privacy leakage, and model robustness, PenTiDef provides a comprehensive advancement over existing defenses in federated intrusion detection systems. A comprehensive comparison of existing defenses is presented in Table 2, illustrating PenTiDef’s effectiveness in addressing poisoning attacks under FL settings.

3 Threat model

3.1 Overview

For this research, we assume that FL-based IDS is constructed with 20 participating collaborators, setting the number of attackers at 10%, 20% and 40% (equivalent to 2, 4, and 8 attackers, respectively). This proportion ensures that the number of attackers is less than half of the total number of participants. The training consisted of 10 rounds, and the attackers executed poisoning attacks from the very first round until the last. Throughout the global model training process, the remaining participants are considered trustworthy. All trainers are required to participate in FL training, contributing to and fully updating their local models.

3.2 Attack strategy

3.2.1 Untargeted attack

1. **Label-flipping attack:** is a form of attack where the attacker intentionally changes the labels of training data samples from correct to incorrect, aiming to distort the model training process and reduce the model’s accuracy in classifying data samples. Our ML/DL model is a binary classifier, with benign samples labeled as 0 and attack traffic samples labeled as 1. We simulate an attacker who flips all these labels to their opposite values.
2. **Weight Scaling Attack:** This attack technique involves the attacker scaling the weights of the local model by a large factor before sending them. The goal of weight scaling is to influence the global model aggregation process, causing undesirable or abnormal changes in the final model. This can lead to a skewed or inaccurate global model, degrading system performance. To simulate this attack, we apply the

formula:

$$\tilde{w}_i = \lambda \cdot w_i$$

where:

- \tilde{w}_i is the scaled weight of the i -th local model.
- w_i is the original weight of the i -th local model.
- λ is the scaling factor, typically a value greater than 1.

3. **Untargeted-Krum** [18]: This attack aims to degrade the performance of the global model without a specific target. The attacker sends manipulated but seemingly benign model parameters to maximize their acceptance by the Krum algorithm. Krum selects the most reliable local model based on the Euclidean distance between model parameters. However, Untargeted-Krum attack attempts to make the malicious parameters resemble benign ones to be selected, harming the global model without easy detection.
4. **Untargeted-Med** [18]: This attack manipulates model parameters based on the maximum and minimum values of the model parameters so that the median value by coordinate moves in the opposite direction.

The goal of Untargeted-Med attacks is to reduce the performance of the global model without a specific target. Attackers can degrade the model’s performance without detection by altering model parameters so that the median coordinate value moves in the opposite direction. This is done by changing parameter values to fall outside the range of benign values.

3.2.2 Targeted attack

1. **Backdoor** [35]: A backdoor attack involves injecting a malicious model into the existing model while maintaining the accuracy of other tasks. This means that the attacked model still performs well on the original tasks, but behaves undesirably when encountering a specific trigger. In our simulation, the backdoor trigger is added to the training data by checking the average value of each sample and changing its label if the average value exceeds a threshold. This can cause the global model to behave unexpectedly when it encounters samples with the trigger during prediction.
2. **GAN poisoning attack** [36]: This involves using a type of artificial neural network to generate new data that resemble real data. A GAN consists of two sub-networks: a **Generator** and a **Discriminator**. The generator creates new data from an input dataset, while the discriminator distinguishes between real and generated data. By introducing fake data, the attacker trains with their malicious local model, thereby degrading and distorting the global model’s classification performance.

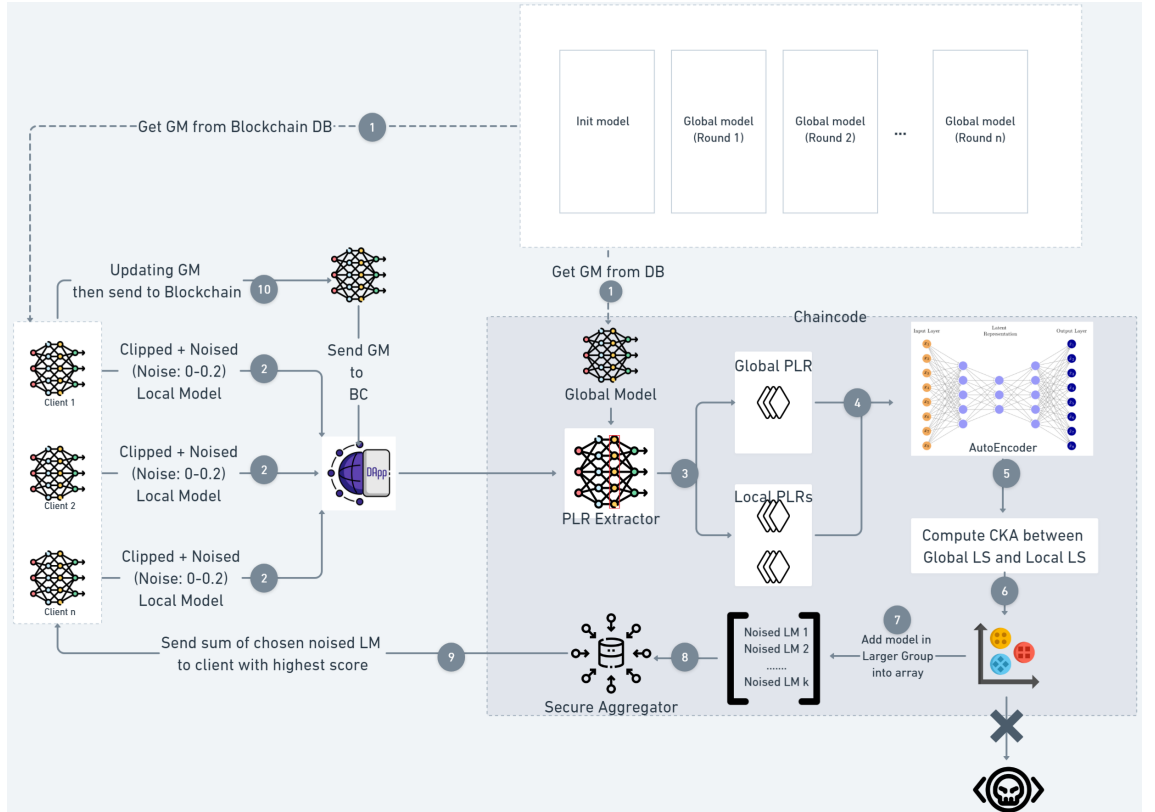


Fig. 1: The PenTiDef architecture for privacy-preserving and anti-poisoning attack mechanisms in DFL-based IDS

4 Proposed architecture

4.1 Design of PenTiDef framework

4.1.1 Architectural components

The architecture of the proposed PenTiDef framework is illustrated in Figure 1, highlighting its novel extension into the domain of decentralized federated learning (DFL) through the integration of blockchain technologies for secure and transparent contribution validation.

Collaborating Parties: These are the distributed participants (e.g., edge devices, institutions) responsible for training their local intrusion detection models on private datasets. Each party periodically uploads its locally trained model weights for validation and selective aggregation.

Blockchain Network: Departing from traditional FL architectures, PenTiDef leverages a permissioned blockchain infrastructure to provide a tamper-evident, verifiable, and decentralized record of model contributions. This network serves not only

as a passive ledger but also hosts smart contracts (chaincode) that autonomously coordinate model evaluation and selection.

Key components of the blockchain-enhanced DFL architecture include:

- *Chaincode*: Implements smart contracts that orchestrate the validation pipeline. It receives perturbed model updates from local parties, verifies their legitimacy using behavioral metrics, and filters out suspicious or malicious contributions before aggregation.
- *PLR Extractor*: Extracts Perturbed Latent Representations (PLRs) from both local and global models. This ensures that only meaningful representational features are used for trustworthiness analysis.
- *AutoEncoder (AE)*: The AE model encodes PLRs into Latent Semantic Representations (LSRs), capturing the core characteristics of benign learning patterns. While this mechanism is inspired by prior work such as Fed-LSAE [20], PenTiDef extends its application by embedding it in a blockchain-driven validation context, enabling fully decentralized trust enforcement.
- *CKA Similarity Module*: Uses Centered Kernel Alignment (CKA) [37] to measure the similarity between local LSRs and the global model’s LSR. Although CKA has been adopted in prior works, its integration into a decentralized and smart contract-managed ecosystem for adversarial detection marks a significant departure from existing centralized approaches.
- *KMeans Clustering Module*: Facilitates unsupervised grouping of model contributions based on their CKA similarity scores. By identifying outlier clusters, the system isolates potentially malicious participants, enhancing robustness even in non-IID or adversarial environments.
- *Secure Aggregator*: Aggregates only the models from nodes identified as benign. It preserves privacy through secure multi-party computation principles, ensuring that individual model contributions remain undisclosed during the aggregation phase, which is especially vital in decentralized setups without a central trusted server.

In summary, unlike traditional FL or semi-decentralized federated schemes, PenTiDef represents a truly decentralized trust framework that leverages blockchain not only as a ledger but as an active orchestrator of security and accountability. This positions PenTiDef as a promising approach for real-world deployment in federated intrusion detection scenarios with minimal central control.

4.1.2 Working principles of PenTiDef

Algorithm 1 details the operational mechanism of the PenTiDef module, which is integrated into the DFL training process of the IDS system model. Specifically, the process to preserve privacy and detect poisoning attacks goes through the following steps:

- *Step 1*: The process begins each round when clients and chaincode access the database to retrieve the current version of the global model. This ensures that all participating parties start with the same base model, creating a uniform foundation for subsequent training and updates.

Algorithm 1 The mechanism of PenTiDef for preventing poisoning attacks

Input: Global weight W ,
A list of n noised local weights $L = \{w_1, w_2, \dots, w_n\}$,
AutoEncoder model AE

Output: Sum of benign local weights W' ,
Index of the most similar local model max_index

▷ PLR Extraction of W and array list L

```
1: for  $i \leftarrow 1$  to  $n$  do
2:    $local\_plr[i] \leftarrow L[i][penultimate\_layer]$ 
3: end for
4:  $global\_plr \leftarrow W[penultimate\_layer]$ 
   ▷ Compute LSR of PLRs using AutoEncoder
5:  $global\_lsr \leftarrow AE.Encoder(global\_plr)$ 
6: for  $i \leftarrow 1$  to  $n$  do
7:    $local\_lsr[i] \leftarrow AE.Encoder(local\_plr[i])$ 
8: end for
9: for  $i \leftarrow 1$  to  $n$  do
10:   $cka[i] \leftarrow CKA(global\_lsr, local\_lsr[i])$ 
11:  if  $cka[i] > cka[max\_index]$  then
12:     $max\_index \leftarrow i$ 
13:  end if
14: end for
   ▷ CKA Score Clustering
15:  $result \leftarrow KMeans(n\_clusters = 2, cka)$ 
16:  $poisoned\_group \leftarrow result.minority\_group$ 
17:  $benign\_group \leftarrow result.majority\_group$ 
   ▷ Aggregated benign local weights
18:  $W' \leftarrow FedAvg(benign\_group)$ 
   return  $W', max\_index$ 
```

- *Step 2:* The collaborative servers train their local models using their respective private datasets. Upon completing the training process, each participant applies noise perturbation to the local model before transmission. The details of this process are provided in **Section 4.2**.
- *Step 3:* As described in **Algorithm 1**, after being sent to the blockchain network, along with the global model, each local model extracts PLR using the PLR Extractor (lines 1-4).
- *Step 4:* The PLR for the global model and n PLRs for the local models are input into the AutoEncoder model architecture to reduce the size of the PLRs and generate LSR (lines 5-11). The main objective of this step is to minimize the instability of the PLR set regarding data characteristics, especially when extracted from heterogeneous datasets. This is crucial in the context where participating organizations train local models in a non-IID data distribution environment.

- *Step 5*: After obtaining a set of LSR, the CKA score is calculated to measure the similarity between the LSR vectors of the local models compared to the PLR vector of the global model. In deciding to use CKA instead of other popular algorithms like Cosine or Euclidean, it is found that CKA can better distinguish the similarity differences between benign models trained on non-IID data [37, 38]. This difference is much smaller than the similarity between benign non-IID models and poisoned models. Therefore, the efficiency in distinguishing and removing the models of malicious actors from the FL learning process is higher, even in the case of heterogeneous data. To implement the CKA similarity scoring, we adopt the **linear kernel variant** due to its computational efficiency and robustness in comparing representations across non-IID data distributions. Let $X \in \mathbb{R}^{n \times d}$ and $Y \in \mathbb{R}^{n \times d}$ denote two latent space representations (LSRs) of local and global models, respectively. The kernel matrices are computed as $K = XX^\top$ and $L = YY^\top$. Both matrices are centered using the standard centering matrix $H = I - \frac{1}{n}\mathbf{1}\mathbf{1}^\top$, producing $K_c = HKH$ and $L_c = HLY$. The final Centered Kernel Alignment (CKA) score is then computed using:

$$\text{CKA}(X, Y) = \frac{\|K_c L_c\|_F^2}{\|K_c K_c\|_F \cdot \|L_c L_c\|_F}$$

where $\|\cdot\|_F$ denotes the Frobenius norm.

Prior to computation, all latent vectors are mean-centered and L2-normalized to ensure numerical stability and eliminate scale effects induced by data heterogeneity and DDP noise.

The rationale for selecting CKA over conventional similarity metrics such as cosine similarity or *Euclidean distance* lies in its capacity to compare structural similarities in high-dimensional representations rather than just vector orientation or distance. In our empirical evaluation, CKA consistently provided better separation between benign and malicious models, especially under non-IID data conditions.

- *Step 6*: Next, after obtaining an array of CKA scores as calculated above, this phase clusters the CKA scores into two separate groups: the majority group and the minority group (lines 12-14). This grouping process helps identify which local models have high consistency with the global model and which have low consistency.
- *Step 7*: For this topic, assuming that the proportion of attackers among the total collaborative servers does not reach 50%, we use the K-Means clustering algorithm to minimize computation costs. Therefore, for the PLRs in the *majority* group, we can classify them as PLRs of benign models. Similarly, conversely, the PLRs in the minority group are classified as malicious and discarded.
- *Step 8*: Once the malicious models have been filtered out, the Secure Aggregator proceeds to combine the remaining benign models. This stage ensures that only trustworthy updates contribute to the global model, while maintaining the confidentiality and integrity of individual local updates during aggregation.
- *Step 9*: After the benign models are aggregated using the FedAvg algorithm, the resulting global model is transmitted to the collaborative server with the highest CKA score, as shown in **Algorithm 2**. This selection strategy ensures that the

most trustworthy participant—whose representation aligns closely with the global model—receives and broadcasts the update promptly and reliably.

- *Step 10*: Finally, the selected party receiving the aggregation result from the Secure Aggregator updates its global model and simultaneously updates this information on the blockchain. This ensures that the entire network of collaborative servers and chaincode has the latest and secured global model.

Algorithm 2 Benign-aware Federated Aggregation in PenTiDef

Input: List of k benign weights $L = \{w_1, w_2, \dots, w_k\}$ selected via CKA-based filtering

Output: Aggregated global weight W'

```

1:  $W' \leftarrow 0$ 
2: for each  $w_i$  in  $L$  do
3:    $\Delta w_i \leftarrow \text{ClientUpdate}(i, w_i)$ 
4:    $W' \leftarrow W' + \Delta w_i$ 
5: end for
6:  $W' \leftarrow \frac{1}{k} W'$ 

7: function ClientUpdate( $i, w$ )
8: for each local epoch  $e = 1, 2, \dots, E$  do
9:   for each batch  $b \in B_i$  do
10:     $w \leftarrow w - \eta \nabla L(b; w)$ 
11:   end for
12: end for
13: return  $\Delta w$ 

```

4.2 DDP with Random Noise Level

Given the decentralized nature of DFL, PenTiDef employs a Distributed Differential Privacy (DDP) mechanism to protect local updates without relying on a trusted server. Each participant perturbs its model parameters before uploading to the blockchain, ensuring privacy at the client level.

We adopt the Gaussian mechanism to realize DDP, defined as:

$$\mathcal{M}_{\text{Gaussian}}(w, \epsilon, \delta) = w + \mathcal{N}(0, \sigma^2)$$

where w is the weight vector of the local model, and $\mathcal{N}(0, \sigma^2)$ is Gaussian noise with variance σ^2 . The privacy budget (ϵ, δ) quantifies the privacy guarantee, while the noise scale σ is calculated as:

$$\sigma = \frac{\sqrt{2 \ln(1.25/\delta)} \cdot \Delta_2}{\epsilon}$$

Here, Δ_2 represents the L_2 sensitivity of the model update function, computed as the maximum difference between updates on adjacent datasets.

To enhance unpredictability and robustness against adversaries, PenTiDef introduces randomness into the selection of σ . Specifically, σ is sampled from a bounded

interval $[0, 0.2]$ at each round, ensuring that noise patterns cannot be reliably inferred while maintaining model utility. This stochasticity prevents free-rider clients from exploiting fixed noise patterns and reinforces protection against reconstruction attacks.

The perturbed model \tilde{w}_i is subsequently used in both latent representation analysis (PLR \rightarrow LSR \rightarrow CKA) and in global model aggregation. Therefore, the noise level must be carefully controlled to strike a balance between privacy and learning performance.

Finally, each client’s noise level σ is recorded as metadata on the blockchain ledger for auditability, without exposing the original model weights. This design ensures full alignment between privacy preservation and decentralized trust in PenTiDef.

4.3 Blockchain Integration in Federated Coordination

In the PenTiDef architecture, blockchain serves as the foundational coordination and verification layer that enables trustless collaboration across decentralized participants. Formally, we define the FL process as a sequence of asynchronous local updates $\{w_i^t\}$ submitted by n clients at each global round t . To ensure integrity and auditability of these updates without relying on a central aggregator, PenTiDef employs a permissioned blockchain network \mathcal{B} , which operates as a decentralized ledger of model transactions.

In our implementation, we deployed the blockchain layer using Hyperledger Fabric, a modular and extensible enterprise-grade DLT platform. The Fabric network is composed of 3 peers and 6 nodes, representing different federated participants. Each peer hosts one or more Fabric nodes that execute chaincode (smart contracts) and maintain a synchronized ledger copy. This distributed setup enhances fault tolerance and decentralization, ensuring that the FL process remains secure and auditable across multiple administrative domains.

Each local update w_i^t is cryptographically referenced on-chain via a unique hash identifier $h(w_i^t)$, where $h(\cdot)$ is a secure, collision-resistant hash function. The blockchain ledger \mathcal{L} maintains an ordered tuple $\langle h(w_i^t), \mathbf{meta}_i^t \rangle$, where \mathbf{meta}_i^t includes metadata such as training round, client ID, differential privacy budget, and aggregated trust score derived from latent space analysis. Rather than storing model weights directly on-chain—which would introduce scalability bottlenecks—PenTiDef delegates parameter storage to an off-chain decentralized storage system. This integration is abstracted through verifiable hash pointers in \mathcal{L} and detailed further in the implementation section.

To regulate participation and prevent unauthorized contribution or manipulation, each client must register within a membership management protocol defined by a smart contract ϕ , which issues identity-bound certificates $(\text{ID}_i, \text{SK}_i)$. These credentials are used to digitally sign model update transactions, ensuring authenticity and accountability. Furthermore, smart contracts orchestrate the model aggregation process by validating model submissions against predefined conditions—such as passing latent space anomaly detection—and applying reward or penalty functions based on client behavior.

Let \mathcal{T} denote the set of all transactions recorded on \mathcal{B} during the training lifecycle. For each valid transaction $\tau \in \mathcal{T}$, the blockchain enforces:

$$\text{VerifySig}(\text{ID}_i, \tau) \wedge \text{ValidateMeta}(\text{meta}_i^t) \Rightarrow \text{Append}(\tau, \mathcal{L})$$

This guarantees that only authorized and verifiably correct updates are admitted into the global learning state. The immutability of \mathcal{L} also provides an auditable history of client participation and model evolution, supporting post-hoc analysis or forensic investigation in the event of adversarial behavior.

Overall, blockchain integration within PenTiDef ensures trustless coordination, secure logging of model contributions, and transparent enforcement of protocol-level logic—effectively replacing the centralized server in traditional FL settings. The actual storage of model parameters is delegated to a decentralized file system, whose integration details are provided in the Section 6.

5 Research Questions and Experimental Design

5.1 Research Questions

In this section, we address the following research questions (RQ):

- **RQ1:** To what extent does the application of Distributed Differential Privacy (DDP) affect the model’s training performance?
- **RQ2:** How does the PenTiDef framework perform under non-IID data distributions, and how does this performance compare to IID settings?
- **RQ3:** How does PenTiDef compare with existing state-of-the-art defense mechanisms in terms of detection accuracy and robustness?
- **RQ4:** How effective is PenTiDef in detecting both untargeted and targeted poisoning attacks under different adversarial conditions?
- **RQ5:** Does PenTiDef achieve cost-efficiency in terms of computational overhead and training time compared to baseline approaches?
- **RQ6:** Is PenTiDef robust across different DL architectures, and does it maintain consistent performance?
- **RQ7:** What is the transaction processing capability of the blockchain coordination layer under different throughput and latency conditions?

5.2 Experimental Scenarios

To address the research questions above, we design four experimental scenarios as follows:

5.2.1 Scenario 1: Impact of DDP on Model Performance (RQ1)

This experiment assesses the effect of applying DDP noise to local models. Specifically, we evaluate PenTiDef with and without DDP under controlled noise levels ($\sigma \in [0, 0.2]$) to determine its impact on convergence and detection accuracy.

5.2.2 Scenario 2: Comparative Evaluation under IID and non-IID Settings (RQ2, RQ3, RQ4, RQ5)

This scenario compares PenTiDef with two representative defense mechanisms—FLARE [19] and FedCC [18]—under both IID and non-IID data distributions. We simulate poisoning attacks (as defined in Section 3.2) with varying adversary ratios (10%, 20%, 40%) and evaluate the models using multiple performance metrics. Training time is also recorded to assess cost-efficiency.

5.2.3 Scenario 3: Cross-Architecture Robustness Evaluation (RQ5, RQ6)

To examine model generalizability, we repeat Scenario 2 using different DL architectures—CNN and SqueezeNet. This allows us to evaluate PenTiDef’s stability across heterogeneous model backbones.

5.2.4 Scenario 4: Blockchain Layer Performance Benchmarking (RQ7)

This scenario evaluates the transaction processing capacity of the Hyperledger-based blockchain layer used for decentralized coordination. We measure latency, throughput, and success rate under increasing transaction loads (5, 20, and 50 TPS) by executing smart contract operations such as model submission, querying, and verification.

6 Implementation and Evaluation metrics

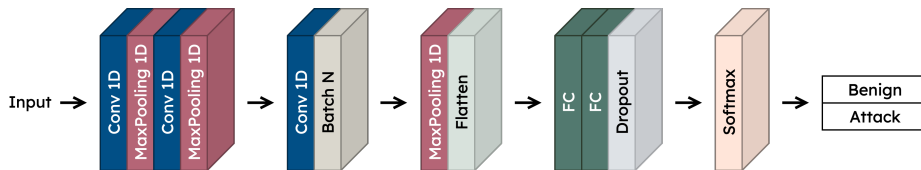


Fig. 2: Details of layers in CNN

6.1 Environmental Setup

In this study, our experimental environment is set up on a computer running Windows OS, equipped with an AMD Ryzen 7 6800HS CPU, 16GB DDR RAM.

In our implementation, the blockchain coordination layer is realized using Hyperledger Fabric, a permissioned blockchain platform that supports modular consensus and fine-grained access control, enabling secure, auditable, and efficient orchestration of decentralized FL processes. For off-chain model parameter storage, PenTiDef integrates the InterPlanetary File System (IPFS) to efficiently manage and retrieve local model updates based on their corresponding hash references maintained on the blockchain ledger.

6.2 Blockchain Architecture and Performance Evaluation Framework

In a Hyperledger Fabric network, multiple organizations collaborate to develop and maintain the blockchain system. Each organization typically operates its own certificate authority (CA), which issues identity certificates to both users and system components. Peer nodes, authenticated through their respective organizations' CAs, maintain copies of the ledger—a distributed and tamper-resistant record of all transactions. These nodes are responsible for validating transactions, executing smart contracts (chaincode), and updating their local ledgers accordingly. In addition to peer nodes, the network incorporates an ordering service that sequences transactions chronologically before committing them to the ledger, ensuring consistency across the system.

Applications interact with the network through a client software development kit, sending transaction requests to peer nodes and invoking smart contracts to perform operations or query the ledger. Transaction proposals are signed using the user's identity certificate, endorsed by selected peer nodes, and then submitted to the ordering service. The ordering service packages proposals into blocks, which are distributed to peer nodes for validation and ledger updates.

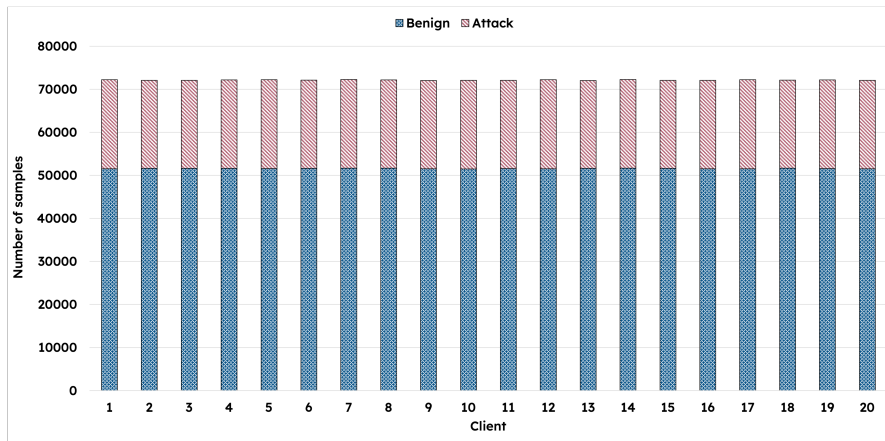
In our study, the network is composed of 3 organizations, each one contains 2 peer nodes. Moreover, to evaluate the network's performance, we employed Hyperledger Caliper, a benchmarking framework developed by the Linux Foundation that provides standardized and trustworthy performance metrics fully compatible with Hyperledger Fabric. Caliper was used to measure key indicators such as transaction throughput (Transactions Per Second—TPS), transaction latency, and system resource utilization (CPU and memory consumption), enabling a comprehensive assessment of the system's deployment efficiency and transaction performance within the Hyperledger Fabric environment.

6.3 Neural Networks for IDS model

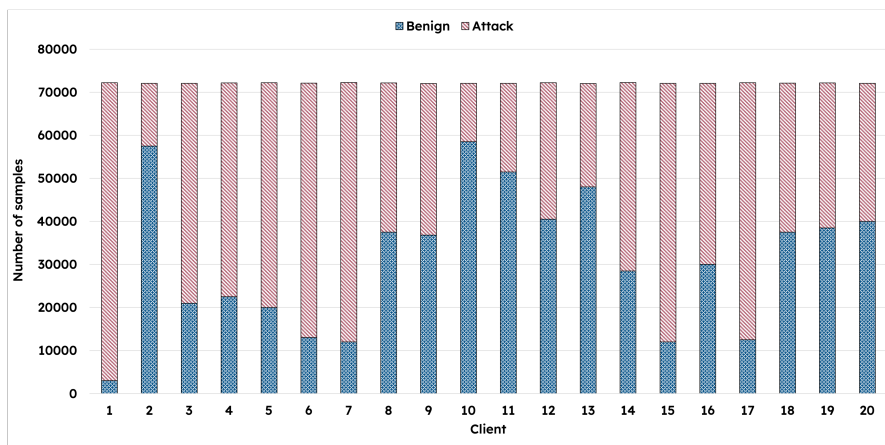
We use a Convolutional Neural Network (CNN) to carry out the experiment. The model comprises one input layer, 11 hidden layers, and one output layer, as shown in **Figure 2**. The input layer processes raw data for feature extraction, while the output layer generates classification results. Our model employs the Adam optimizer and the ReLU activation function. Training involves a batch size of 1024 and runs for 5 epochs, with the FL simulation incorporating 20 clients.

6.4 Dataset

Our benchmarking scenarios utilize two datasets: Edge-IIoTSet [39] and CIC-IDS2018 [40]. After preprocessing, the Edge-IIoTSet dataset consists of 95 features and one label column, with a labeling ratio of roughly 71.4% benign data and 28.6% attack data. In the case of the CIC-IDS2018 dataset, there are 71 features and a label column after preprocessing, with approximately 42.6% benign data and 57.4% attack data. We assign 30% of each dataset for testing to ensure an unbiased evaluation of the performance of the model, while the remaining 70% was evenly distributed among the



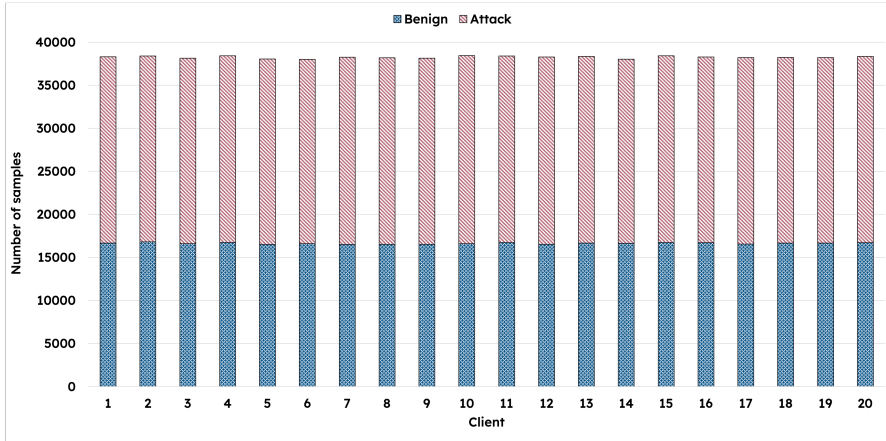
(a) IID



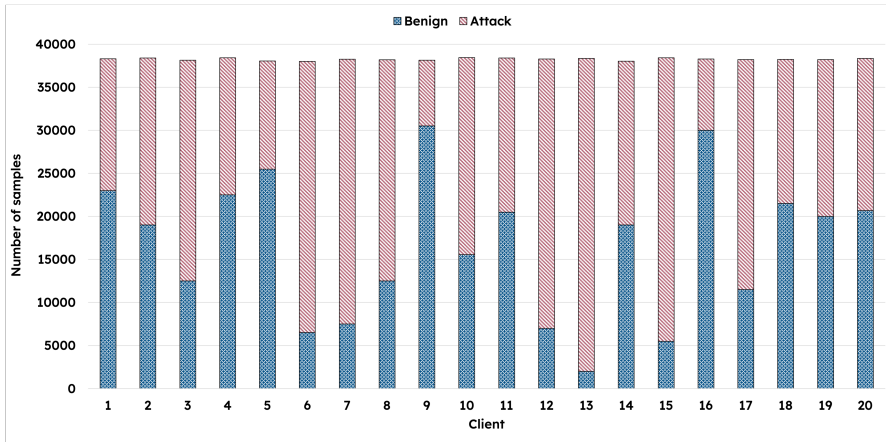
(b) non-IID

Fig. 3: Data distribution of the Edge-IIoTSet dataset under IID and non-IID scenarios

collaborating machines. In addition, we have divided the datasets into IID and non-IID subsets to thoroughly evaluate the performance and robustness of the PenTiDef model under different data distributions. In doing so, our objective is to demonstrate the model's capability to maintain high accuracy and stability, regardless of the underlying data distribution, further validating its applicability and reliability in diverse FL applications. The details of the data distribution for the two datasets on iid and non-iid condition are shown in **Figure 3** and **Figure 4**.



(a) IID



(b) non-IID

Fig. 4: Data distribution of the CIC-IDS2018 dataset under IID and non-IID scenarios

6.5 Evaluation Metrics

To evaluate the effectiveness of the proposed PenTiDef framework, we adopt four standard metrics commonly used in binary classification tasks: Accuracy, Precision, Recall, and F1-Score.

Accuracy measures the overall proportion of correctly classified samples. *Precision* reflects the proportion of correctly predicted positive instances among all predicted positives. *Recall* quantifies the model’s ability to identify actual positive instances. *F1-Score* represents the harmonic mean of Precision and Recall, offering a balanced measure in cases of class imbalance.

These metrics are derived from the confusion matrix composed of true positives, true negatives, false positives, and false negatives. They provide a comprehensive

view of model performance in distinguishing between benign and malicious traffic. In addition, we employ the *Centered Kernel Alignment (CKA) Score* to measure the similarity between latent representations of local and global models. This metric is particularly useful for evaluating the consistency of feature space across participants and identifying anomalies introduced by poisoned updates. Based on this measure, we can distinguish and eliminate poisoned models from the update process. A higher CKA score indicates that the local model is closer to the global model.

7 Experimental Results and Analysis

7.1 Result 1 (Answer to Scenario 1): PenTiDef maintains high performance under DDP with minimal accuracy degradation

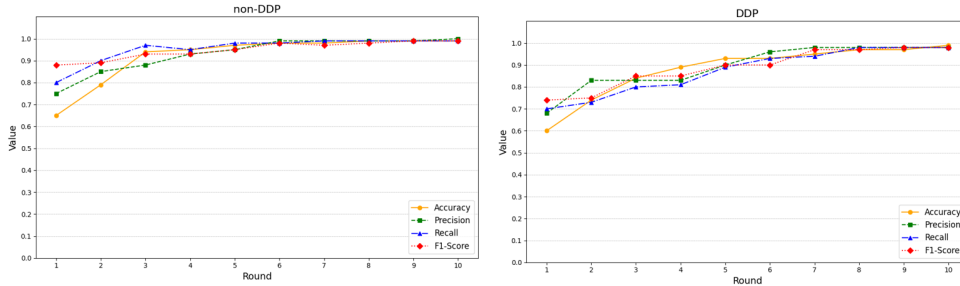


Fig. 5: Comparison of training results with and without applying DDP

Table 3: Performance comparison of defense methods on IID datasets for detecting untargeted attacks

Dataset	Attack	Adversaries 10%				Adversaries 20%				Adversaries 40%			
		No-Def	Flare	FedCC	PenTiDef	No-Def	Flare	FedCC	PenTiDef	No-Def	Flare	FedCC	PenTiDef
CIC-IDS2018	LF	0.77	0.96	0.96	0.97	0.75	0.93	0.95	0.96	0.71	0.92	0.95	0.96
	WS	0.76	0.95	0.95	0.96	0.76	0.97	0.95	0.96	0.68	0.92	0.96	0.96
	Un-Krum	0.73	0.95	0.97	0.96	0.72	0.95	0.96	0.97	0.64	0.96	0.88	0.93
Edge-IIoTset	Un-Med	0.73	0.96	0.96	0.98	0.65	0.95	0.93	0.98	0.67	0.91	0.92	0.97
	LF	0.65	0.99	0.98	0.98	0.63	0.92	0.96	0.97	0.57	0.88	0.88	0.92
	WS	0.64	0.95	0.96	0.95	0.63	0.95	0.97	0.95	0.58	0.91	0.88	0.95
Edge-IIoTset	Un-Krum	0.67	0.94	0.94	0.95	0.67	0.98	0.91	0.96	0.58	0.91	0.87	0.93
	Un-Med	0.73	0.94	0.96	0.97	0.64	0.88	0.93	0.99	0.56	0.88	0.88	0.95

The performance of the PenTiDef model under two conditions, without applying DDP (non-DDP) and with applying DDP, is shown in **Figure 5**, demonstrating a distinct difference in the initial stage. Initially, when applying DDP, the training performance is lower than non-DDP due to DDP adding noise to the model to protect privacy, resulting in a slower convergence rate.

Table 4: Performance comparison of defense methods on IID datasets for detecting targeted attacks

Dataset	Attack	Adversaries 10%				Adversaries 20%				Adversaries 40%			
		No-Def	Flare	FedCC	PenTiDef	No-Def	Flare	FedCC	PenTiDef	No-Def	Flare	FedCC	PenTiDef
CIC-IDS2018	GAN-SL	0.68	0.96	0.95	0.97	0.67	0.93	0.95	0.97	0.57	0.90	0.93	0.94
	GAN-ML	0.73	0.97	0.96	0.96	0.73	0.95	0.96	0.96	0.63	0.93	0.96	0.97
	GAN-Con	0.74	0.95	0.96	0.97	0.74	0.95	0.96	0.97	0.56	0.88	0.93	0.95
	BD	0.69	0.96	0.96	0.97	0.69	0.96	0.96	0.97	0.59	0.94	0.92	0.94
Edge-IIoTset	GAN-SL	0.58	0.93	0.92	0.92	0.58	0.93	0.92	0.93	0.58	0.93	0.93	0.94
	GAN-ML	0.63	0.93	0.94	0.93	0.63	0.93	0.95	0.93	0.63	0.92	0.93	0.94
	GAN-Con	0.60	0.92	0.92	0.93	0.60	0.96	0.90	0.95	0.60	0.93	0.92	0.94
	BD	0.59	0.92	0.93	0.93	0.59	0.88	0.91	0.93	0.59	0.94	0.94	0.95

Table 5: Performance comparison of defense methods on non-IID datasets for detecting untargeted attacks

Dataset	Attack	Adversaries 10%				Adversaries 20%				Adversaries 40%			
		No-Def	Flare	FedCC	PenTiDef	No-Def	Flare	FedCC	PenTiDef	No-Def	Flare	FedCC	PenTiDef
CIC-IDS2018	LF	0.36	0.92	0.93	0.95	0.46	0.91	0.93	0.94	0.41	0.90	0.92	0.93
	WS	0.42	0.93	0.93	0.94	0.47	0.93	0.91	0.92	0.41	0.90	0.92	0.93
	Un-Krum	0.40	0.90	0.93	0.94	0.44	0.92	0.92	0.93	0.40	0.92	0.84	0.89
	Un-Med	0.43	0.91	0.91	0.94	0.44	0.92	0.92	0.93	0.40	0.87	0.88	0.95
Edge-IIoTset	LF	0.37	0.91	0.90	0.90	0.37	0.92	0.93	0.94	0.37	0.84	0.85	0.88
	WS	0.44	0.89	0.91	0.91	0.41	0.91	0.93	0.92	0.44	0.87	0.86	0.91
	Un-Krum	0.46	0.90	0.90	0.91	0.43	0.94	0.89	0.92	0.44	0.87	0.83	0.89
	Un-Med	0.51	0.91	0.89	0.94	0.40	0.84	0.89	0.95	0.42	0.84	0.84	0.91

In the early training rounds, the PenTiDef model with DDP shows slower growth and lower metrics compared to non-DDP. However, in the subsequent rounds, the DDP model gradually converges and reaches stability, though still approximately 0.01 lower than non-DDP across all criteria.

These results demonstrate that PenTiDef maintains high and stable performance even when applying DDP, reflecting a balance between security and performance. PenTiDef is capable of adapting and operating efficiently in decentralized FL environments, ensuring security while maintaining high accuracy in detecting network threats.

7.2 Result 2 (Answer to Scenario 2): PenTiDef outperforms state-of-the-art defenses across IID and non-IID data under multiple poisoning attacks

Training on IID Datasets The results in Table 3 demonstrate that PenTiDef outperforms other models in most cases for untargeted attacks. Specifically, PenTiDef consistently achieves the highest or near-highest values in evaluation criteria such as Accuracy, Precision, Recall, and F1-Score. This is evident across all levels of adversarial presence, showing that PenTiDef maintains stable and superior performance even as the adversary rate increases. PenTiDef’s performance remains robust when facing various types of attacks, especially in cases like Untargeted-Med and Un-Krum, where

it frequently achieves the highest performance. This highlights the effectiveness of PenTiDef in detecting and defending against untargeted poisoning attacks.

Table 4 lists the parameters of the defense methods against targeted attacks. Overall, all three defense methods show a comparison to detecting untargeted attacks. This can be explained by the fact that targeted attacks are harder to detect. Targeted attacks are designed specifically for each target, utilizing evasion techniques, exploiting zero-day vulnerabilities, and employing APTs. Attackers often patiently gather intelligence, maintain long-term persistence, and leverage insider threats, making them significantly more challenging to identify. In contrast, untargeted attacks are more widespread, relying on common tools and techniques, which makes them easier to detect. Targeted attacks often have sophisticated characteristics and specific goals, such as skewing predictions for a particular type of input without significantly altering the model’s overall performance. These small and subtle changes require defense methods to be highly sensitive. Nonetheless, our model still achieves the highest performance in most of these attacks.

Table 6: Performance comparison of defense methods on non-IID datasets for detecting targeted attacks

Dataset	Attack	Adversaries 10%				Adversaries 20%				Adversaries 40%			
		No-Def	Flare	FedCC	PenTiDef	No-Def	Flare	FedCC	PenTiDef	No-Def	Flare	FedCC	PenTiDef
CIC-IDS2018	GAN-SL	0.55	0.91	0.91	0.92	0.45	0.91	0.91	0.92	0.52	0.88	0.88	0.89
	GAN-ML	0.53	0.92	0.94	0.92	0.45	0.91	0.93	0.92	0.50	0.89	0.91	0.89
	GAN-Con	0.53	0.94	0.94	0.95	0.46	0.93	0.93	0.50	0.91	0.91	0.92	0.92
	BD	0.54	0.93	0.93	0.95	0.46	0.93	0.92	0.93	0.51	0.90	0.90	0.92
Edge-IIoTset	GAN-SL	0.55	0.91	0.89	0.89	0.46	0.91	0.89	0.90	0.52	0.88	0.86	0.86
	GAN-ML	0.56	0.91	0.93	0.91	0.46	0.91	0.93	0.90	0.53	0.88	0.90	0.88
	GAN-Con	0.56	0.92	0.92	0.93	0.44	0.92	0.92	0.93	0.53	0.89	0.89	0.90
	BD	0.55	0.91	0.91	0.95	0.44	0.91	0.91	0.94	0.52	0.88	0.88	0.92

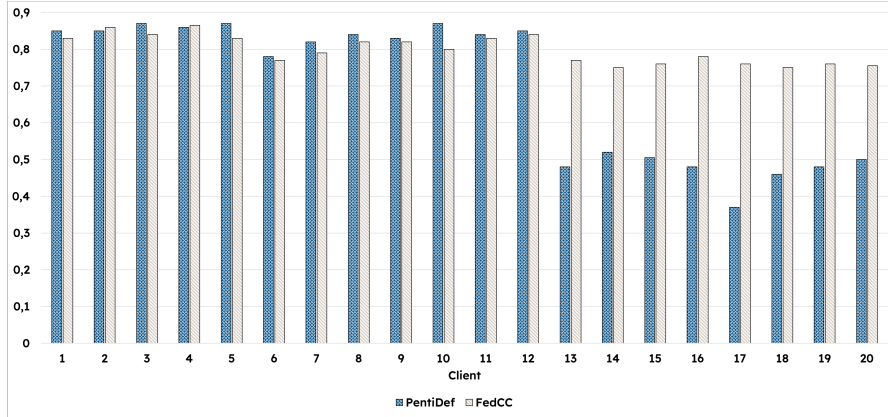


Fig. 6: Similarity comparison between the latent space of the global model and each local model’s latent space using CKA scores in PenTiDef and FedCC.

To explain the stability in classifying benign and malicious models, as shown in **Figure 6**, we have compiled the CKA scores for each participant with an attacker ratio of 40% (the last 8 collaborators) using the Untargeted-Krum attack method. These figures were recorded after the final training round. We compare the CKA scores of the two modules, PenTiDef and the module using a similar CKA scoring method, FedCC [18].

It is easily noticeable that there is a significant difference between the CKA scores of benign and malicious LSRs compared to the LSR of the global model. For collaborators from clients 1 to 12 (assumed to be benign), PenTiDef maintains a high level of similarity with CKA scores mostly above 0.8, demonstrating its ability to maintain stability in identifying benign models. On the contrary, the CKA scores for collaborators from clients 13 to 20 (assumed to be malicious) show a significant decline, mostly below 0.6, with some even below 0.5. This indicates that PenTiDef can effectively distinguish between benign and malicious models, even with an attacker ratio of 40%. Meanwhile, FedCC does not exhibit a clear distinction like PenTiDef, resulting in poorer classification performance. This explains why PenTiDef achieves higher performance in most scenarios compared to FedCC.

Training on non-IID Dataset For the case of training on the non-IID heterogeneous dataset, the data distribution among the 20 collaborating models is divided as shown in **Figure 3b** and **Figure 4b**. Similar to the previous case, the following scenarios are simulated with attacker ratios of 10%, 20%, and 40%. Using a non-IID dataset is crucial because, in real-world FL scenarios, data across different clients is inherently non-IID due to variations in user behavior, device environments, and data collection methods. This non-uniformity presents a greater challenge for defense mechanisms, as the differences in local data distributions can lead to model divergence and increased vulnerability to adversarial manipulations. Moreover, non-IID data can obscure attack patterns, making it harder for defenses to differentiate between natural variations in data and malicious manipulations. The reason for distributing the

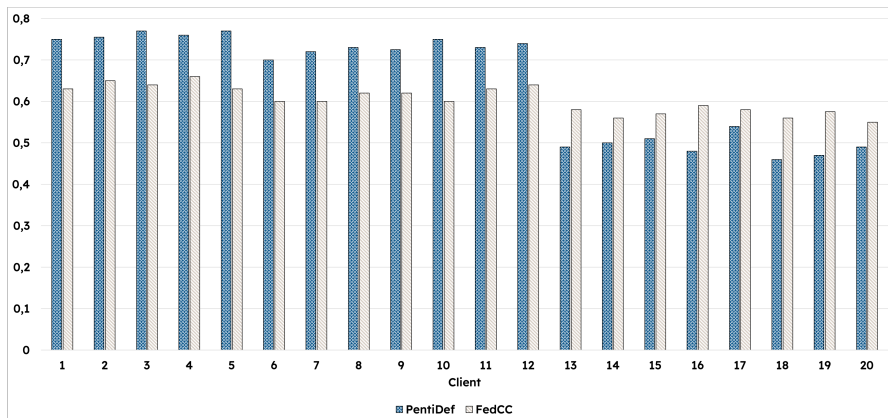


Fig. 7: Compare the similarity between the latent space of the global model and each local model’s latent space using CKA scores in PenTiDef and FedCC.

dataset in this manner is to clarify the differences between the defense methods in distinguishing malicious models when trained on a non-IID dataset. Regarding the results summarized in **Table 5**, it can be observed that due to the influence of the heterogeneous data distribution, the performance results of all three defense modules experience a slight decline. However, our PenTiDef model still achieves the highest performance in most attack scenarios.

Table 6 shows us that PenTiDef remains the model with the most stable performance compared to the other two attack methods, although all three modules experience a decrease in accuracy due to the influence of the non-IID dataset. Specifically, PenTiDef often achieves the highest or near-highest values in most attacks, such as LF, WS, Untargeted-Krum, and Untargeted-Med. This demonstrates PenTiDef’s good capability in distinguishing between benign and malicious models. Even as the ratio of attackers increases, PenTiDef maintains high performance, showing the stability and effectiveness of this method in protecting the system from poisoning attacks. Compared to other methods, PenTiDef always shows a clear difference in metrics. PenTiDef effectively preserves this consistency by ensuring that benign models retain high CKA scores while isolating adversarial updates. In contrast, FedCC struggles to maintain stable CKA scores, particularly in non-IID environments. The uneven data distribution introduces variations in local model updates, leading to inconsistencies that FedCC fails to manage effectively. This lack of stability causes difficulties in distinguishing between benign and malicious models, ultimately reducing FedCC’s detection accuracy.

In summary, PenTiDef stands out as a robust and reliable defense method in protecting distributed ML systems from poisoning attacks. Similar to the statistics in the IID case, targeted attacks in the non-IID case also slightly reduce the performance of all three modules. As seen in Figure 7, due to the impact of the uneven data distribution, the CKA scores for the benign clients have decreased (by approximately 0.1). The CKA scores of FedCC show a lack of stability and clarity in classifying malicious and benign models. This explains why the PenTiDef model has higher performance in most scenarios compared to FedCC.

Finally, to address the question of cost efficiency, **Table 7** summarizes the training time of each defense model. It can be seen that our PenTiDef model has a significantly

Table 7: Average training time on different datasets with different models

Dataset	Model	Training Time
CIC-IDS2018	Flare	3,907s ~ 01h 06m
	FedCC	2,460s ~ 41m
	PenTiDef	1,988s ~ 33m
Edge-IIoTset	Flare	4,395s ~ 1h 15m
	FedCC	2,825s ~ 47m
	PenTiDef	1,869s ~ 31m

Table 8: Performance Comparison of the PenTiDef module on the CIC-IDS2018 and Edge-IIoTset datasets with two DL models, CNN and SqueezeNet (untargeted attack)

Dataset	Attack	10% adv		20% adv		40% adv	
		CNN	SqueezeNet	CNN	SqueezeNet	CNN	SqueezeNet
IID							
CIC-IDS2018	LF	0.97	0.98	0.97	0.98	0.94	0.96
	WS	0.96	0.95	0.96	0.97	0.96	0.97
	Un-Krum	0.96	0.97	0.97	0.98	0.93	0.94
	Un-Med	0.98	0.97	0.97	0.96	0.97	0.98
Edge-IIoTset	LF	0.98	0.97	0.97	0.98	0.92	0.95
	WS	0.98	0.97	0.95	0.96	0.95	0.96
	Un-Krum	0.94	0.95	0.93	0.94	0.89	0.90
	Un-Med	0.98	0.97	0.99	0.98	0.95	0.97
non-IID							
CIC-IDS2018	LF	0.95	0.97	0.94	0.95	0.93	0.95
	WS	0.94	0.93	0.92	0.94	0.93	0.94
	Un-Krum	0.94	0.92	0.93	0.95	0.95	0.94
	Un-Med	0.94	0.93	0.93	0.92	0.95	0.94
Edge-IIoTset	LF	0.90	0.89	0.94	0.93	0.93	0.94
	WS	0.91	0.92	0.92	0.91	0.91	0.90
	Un-Krum	0.91	0.92	0.92	0.90	0.89	0.90
	Un-Med	0.94	0.95	0.95	0.93	0.91	0.90

faster training time compared to the other two models, namely FedCC and FLARE. This can be explained as follows:

- Firstly, the FLARE model uses an algorithm to compute the distance between two PLR vectors. Due to the complexity of this algorithm, FLARE has the slowest training time compared to the other two defense models.
- Secondly, the FedCC model operates more similarly to our model than FLARE. However, FedCC calculates similarity based on PLRs using CKA scores, whereas our model computes it based on LSRs extracted from PLRs through an AE.

Therefore, our model achieves the fastest training time, addressing the issue of resource cost and enhancing scalability in distributed FL environments.

7.3 Result 3 (Answer to Scenario 3): PenTiDef demonstrates model-agnostic robustness across CNN and SqueezeNet architectures

For this scenario, we conduct experiments on the attack scenarios to test the performance of the PenTiDef module. This time, we conduct the experiments on two DL models, including CNN and SqueezeNet. This aims to evaluate the detection and

Table 9: Performance comparison of the PenTiDef module on the CIC-IDS2018 and Edge-IIoTset datasets with two DL models, CNN and SqueezeNet (untargeted attack)

Dataset	Attack	10% adv		20% adv		40% adv	
		CNN	SqueezeNet	CNN	SqueezeNet	CNN	SqueezeNet
IID							
CIC-IDS2018	GAN-SL	0.97	0.96	0.97	0.97	0.94	0.95
	GAN-ML	0.96	0.95	0.96	0.97	0.97	0.96
	GAN-Con	0.97	0.96	0.97	0.98	0.95	0.96
	BD	0.97	0.96	0.97	0.96	0.94	0.95
Edge-IIoTset	GAN-SL	0.92	0.93	0.93	0.94	0.95	0.94
	GAN-ML	0.93	0.94	0.93	0.94	0.95	0.94
	GAN-Con	0.93	0.95	0.95	0.94	0.95	0.94
	BD	0.95	0.97	0.97	0.96	0.95	0.94
non-IID							
CIC-IDS2018	GAN-SL	0.92	0.93	0.94	0.93	0.92	0.93
	GAN-ML	0.92	0.91	0.92	0.91	0.92	0.94
	GAN-Con	0.95	0.93	0.93	0.94	0.95	0.94
	BD	0.95	0.93	0.93	0.94	0.95	0.94
Edge-IIoTset	GAN-SL	0.89	0.88	0.89	0.90	0.89	0.90
	GAN-ML	0.91	0.90	0.91	0.90	0.91	0.92
	GAN-Con	0.93	0.92	0.92	0.93	0.93	0.90
	BD	0.95	0.94	0.95	0.94	0.95	0.96

Table 10: Benchmark results of the Hyperledger Fabric network with 5000 transactions

5 transactions/s							
Name	Succ	Fail	Send Rate (TPS)	Max Latency (s)	Min Latency (s)	Avg Latency (s)	Throughput (TPS)
CreateModel	5000	0	28.1	2.10	0.03	0.21	28.0
QueryAllModels	5000	0	64.1	0.29	0.04	0.10	64.1
QueryLastModel	5000	0	127.0	0.28	0.02	0.05	126.9
QueryModelsBySelectedClientID	5000	0	114.4	0.25	0.02	0.06	114.3
QueryModelsByModelIndex	5000	0	97.8	0.34	0.02	0.06	97.7
QueryModelsByAdversaryClientID	5000	0	86.4	0.49	0.02	0.07	86.4
QueryModelsByBenignClientID	5000	0	78.9	0.25	0.02	0.08	78.9
20 transactions/s							
Name	Succ	Fail	Send Rate (TPS)	Max Latency (s)	Min Latency (s)	Avg Latency (s)	Throughput (TPS)
CreateModel	5000	0	86.5	2.09	0.03	0.12	84.5
QueryAllModels	5000	0	82.1	0.32	0.04	0.17	82.1
QueryLastModel	5000	0	158.8	0.27	0.02	0.10	158.6
QueryModelsBySelectedClientID	5000	0	151.1	0.28	0.02	0.10	151.0
QueryModelsByModelIndex	5000	0	177.7	0.22	0.02	0.09	177.5
QueryModelsByAdversaryClientID	5000	0	129.8	0.53	0.02	0.10	129.6
QueryModelsByBenignClientID	5000	0	113.9	0.46	0.02	0.12	113.8

Table 11: Benchmark results of the Hyperledger Fabric network with 10000 transactions

5 transactions/s							
Name	Succ	Fail	Send Rate (TPS)	Max Latency (s)	Min Latency (s)	Avg Latency (s)	Throughput (TPS)
CreateModel	10000	0	27.6	2.09	0.02	0.22	27.5
QueryAllModels	10000	0	32.8	0.45	0.07	0.18	32.8
QueryLastModel	10000	0	69.9	0.25	0.03	0.09	69.9
QueryModelsBySelectedClientID	10000	0	57.2	0.36	0.04	0.12	57.2
QueryModelsByModelIndex	10000	0	67.7	0.25	0.03	0.10	67.7
QueryModelsByAdversaryClientID	10000	0	47.0	0.50	0.03	0.15	47.0
QueryModelsByBenignClientID	10000	0	48.9	0.43	0.04	0.13	48.9
20 transactions/s							
Name	Succ	Fail	Send Rate (TPS)	Max Latency (s)	Min Latency (s)	Avg Latency (s)	Throughput (TPS)
CreateModel	10000	0	33.1	2.07	0.03	0.11	33.7
QueryAllModels	10000	0	39.4	0.67	0.07	0.35	39.4
QueryLastModel	10000	0	91.5	0.45	0.04	0.16	91.5
QueryModelsBySelectedClientID	10000	0	43.9	1.23	0.05	0.36	43.9
QueryModelsByModelIndex	10000	0	71.4	0.55	0.03	0.21	71.4
QueryModelsByAdversaryClientID	10000	0	45.9	0.97	0.05	0.34	45.9
QueryModelsByBenignClientID	10000	0	47.4	1.00	0.06	0.31	47.4

defense capabilities of PenTiDef on different neural network architectures, thereby determining the stability and effectiveness of the module in various conditions and environments. We conduct experiments on both IID and non-IID cases with (**Table 8**) and targeted attacks (**Table 9**). Similar to scenario 3, the model performs most stably in detecting untargeted attacks on the IID dataset and shows the most fluctuation in the non-IID dataset with targeted attacks.

Based on the statistics tables, the CNN model often achieves higher or equal results compared to SqueezeNet in many different attack scenarios. This indicates that CNN tends to perform more effectively than SqueezeNet in the tested scenarios. However, both models have good detection and defense capabilities, but the stability and effectiveness of the model can be influenced by the type of attack and the data structure used.

Notably, our PenTiDef module has demonstrated stability and flexibility by performing well across various DL models. This shows that PenTiDef not only has strong detection and defense capabilities but can also be flexibly applied to different neural network architectures. The ability to adapt to different models and maintain stable performance proves that PenTiDef is a comprehensive and effective defense solution in protecting DFL-IDS from potential attacks.

7.4 Result 4 (Answer to Scenario 4): The blockchain coordination layer remains efficient and stable under increasing transaction loads

In each evaluation, we executed all the tasks defined in the chaincode to interact with the system, including: CreateModel, GetAllModels, GetLastModel, QueryModelsBySelectedClientID, QueryModelsByModelIndex, QueryModelsByAdversaryClientID, QueryModelsByBenignClientID. Transactions are sent continuously, increasing from 5 to 20 transactions per second, to the system for evaluation.

Tables 10 and 11 present the benchmark results of the Hyperledger Fabric network with 5000 and 10000 transactions. In terms of stability, both tables show the network’s stability, with all transactions being successful. As the number of transactions increased from 5000 to 10000, the sending rate tended to decrease, especially at the rate of 5 transactions per second. The average and maximum latency slightly increased with the higher number of transactions, likely due to the heavier load on the network. The throughput remained relatively high and stable, demonstrating the good performance of the Hyperledger Fabric network in handling transactions. Overall, the Hyperledger Fabric network showed good performance at both load levels of 5000 and 10000 transactions, with all transactions being successful and high throughput.

8 Discussion

The experimental results presented in this study demonstrate that PenTiDef offers significant improvements in both detection accuracy and system robustness compared to state-of-the-art defenses such as FLARE and FedCC. The framework effectively detects both targeted and untargeted poisoning attacks in decentralized environments and maintains performance stability even under non-IID data distributions and high adversary ratios. Notably, PenTiDef achieves this without relying on auxiliary datasets or prior assumptions about the number of malicious participants, which enhances its scalability and practical applicability.

Furthermore, the integration of blockchain-based coordination contributes to system transparency, immutability, and trust management without introducing notable communication overhead. The observed training efficiency—in terms of reduced computation time and convergence behavior—highlights the benefit of combining latent-space representation with AutoEncoder compression and CKA-based similarity scoring.

However, several limitations remain. First, the current implementation is restricted to binary classification, which limits its ability to distinguish between different types of network attacks. Extending PenTiDef to multi-class or multi-label intrusion detection is essential for practical deployments. Second, although PenTiDef demonstrates resilience against common poisoning attacks, more adaptive and stealthy adversaries—such as model inversion or semantic backdoors—require further investigation. Third, the randomized noise injection mechanism in DDP, while effective for privacy protection, may become a vulnerability under free-rider strategies where malicious clients inject excessive noise without contributing meaningful updates.

To further strengthen the framework, future work should incorporate statistical attack detectors for advanced threats, adopt adaptive noise tuning mechanisms to balance privacy and model utility, and explore explainable AI (XAI) methods to provide insights into model decisions. Additionally, a more comprehensive cost-benefit analysis of the blockchain layer—considering transaction throughput, latency under scale, and resource constraints—would offer practical guidelines for deployment in real-world settings.

In summary, while PenTiDef addresses several core limitations of current FL-based IDS defenses, continued refinement and real-world validation will be critical to establishing it as a viable solution for collaborative cybersecurity in IoMT, edge networks, and other distributed critical infrastructures.

9 Conclusion and Future Directions

This study introduces PenTiDef, a novel framework designed to enhance the robustness and privacy of decentralized federated intrusion detection systems (DFL-IDS) against poisoning attacks. By integrating Distributed Differential Privacy (DDP) and latent space-based anomaly detection, PenTiDef effectively mitigates gradient-based privacy leakage and identifies malicious updates through AutoEncoder-compressed representations and CKA-based similarity scoring. Furthermore, the incorporation of blockchain-based decentralized coordination strengthens system transparency and trustworthiness by eliminating reliance on centralized aggregators.

Experimental results on two benchmark datasets, CIC-IDS2018 and Edge-IIoTSet, under IID and non-IID conditions, confirm the superiority of PenTiDef over existing approaches such as FLARE and FedCC in terms of accuracy, resilience, and computational efficiency. The framework demonstrates robust performance even in adversarial settings with up to 40% malicious participants.

Despite its effectiveness, PenTiDef currently focuses on binary classification and assumes a limited set of attack types. Future work will aim to extend the framework to support multi-class intrusion detection, explore more sophisticated and stealthy poisoning strategies, and develop mechanisms to counteract free-rider behavior that may exploit the DDP mechanism. These directions will further enhance the applicability of PenTiDef to real-world federated security applications in highly dynamic and heterogeneous environments. In particular, PenTiDef holds strong potential for deployment in Internet of Medical Things (IoMT) and smart edge computing environments, where privacy preservation, decentralization, and real-time adaptability are critical. The proposed architecture may also serve as a foundation for secure collaborative learning infrastructures in emerging cyber-physical systems.

References

- [1] Agrawal, S., Sarkar, S., Aouedi, O., Yenduri, G., Piamrat, K., Bhattacharya, S., Maddikunta, P.K.R., Gadekallu, T.R.: Federated Learning for Intrusion Detection System: Concepts, Challenges and Future Directions (2021)

- [2] Khan, L.U., Saad, W., Han, Z., Hossain, E., Hong, C.S.: Federated Learning for Internet of Things: Recent Advances, Taxonomy, and Open Challenges (2021)
- [3] Hu, Y., Zhou, Y., Xiao, J., Wu, C.: GFL: A Decentralized Federated Learning Framework Based On Blockchain (2021)
- [4] Qu, Y., Uddin, M.P., Gan, C., Xiang, Y., Gao, L., Yearwood, J.: Blockchain-enabled federated learning: A survey. *ACM Computing Surveys* **55**(4), 1–35 (2022)
- [5] Lyu, L., Yu, H., Ma, X., Chen, C., Sun, L., Zhao, J., Yang, Q., Yu, P.S.: Privacy and robustness in federated learning: Attacks and defenses. *IEEE Transactions on Neural Networks and Learning Systems*, 1–21 (2022) <https://doi.org/10.1109/TNNLS.2022.3216981>
- [6] Fang, H., Qian, Q.: Privacy preserving machine learning with homomorphic encryption and federated learning. *Future Internet* **13**(4) (2021)
- [7] Liu, F., Zheng, Z., Shi, Y., Tong, Y., Zhang, Y.: A survey on federated learning: a perspective from multi-party computation. *Frontiers of Computer Science* **18**(1), 181336 (2024)
- [8] Kalapaaking, A.P., Khalil, I., Yi, X.: Blockchain-based federated learning with smpc model verification against poisoning attack for healthcare systems. *IEEE Transactions on Emerging Topics in Computing* **12**(1), 269–280 (2024) <https://doi.org/10.1109/TETC.2023.3268186>
- [9] Mohassel, P., Zhang, Y.: SecureML: A System for Scalable Privacy-Preserving Machine Learning. *Cryptology ePrint Archive*, Paper 2017/396 (2017)
- [10] Li, X., Qu, Z., Zhao, S., Tang, B., Lu, Z., Liu, Y.: Lomar: A local defense against poisoning attack on federated learning. *IEEE Transactions on Dependable and Secure Computing* **20**(1), 437–450 (2021)
- [11] Yan, B., Jiang, X., Chen, Y., Gao, C., Liu, X.: Afl-cs: Asynchronous federated learning with cosine similarity-based penalty term and aggregation. In: 2023 IEEE 29th International Conference on Parallel and Distributed Systems (ICPADS), pp. 46–53 (2023). <https://doi.org/10.1109/ICPADS60453.2023.00016>
- [12] Jithish, J., Alangot, B., Mahalingam, N., Yeo, K.S.: Distributed anomaly detection in smart grids: A federated learning-based approach. *IEEE Access* **11**, 7157–7179 (2023) <https://doi.org/10.1109/ACCESS.2023.3237554>
- [13] Zhu, H., Xu, J., Liu, S., Jin, Y.: Federated learning on non-iid data: A survey. *Neurocomputing* **465**, 371–390 (2021)
- [14] Zhao, Z., Feng, C., Hong, W., Jiang, J., Jia, C., Quek, T.Q., Peng, M.: Federated

- learning with non-iid data in wireless networks. *IEEE Transactions on Wireless communications* **21**(3), 1927–1942 (2021)
- [15] Li, C.-J., Huang, P.-H., Ma, Y.-T., Hung, H., Huang, S.-Y.: Robust aggregation for federated learning by minimum γ -divergence estimation. *Entropy* **24**(5), 686 (2022)
- [16] Li, S., Ngai, E., Voigt, T.: Byzantine-robust aggregation in federated learning empowered industrial iot. *IEEE Transactions on Industrial Informatics* **19**(2), 1165–1175 (2021)
- [17] Pillutla, K., Kakade, S.M., Harchaoui, Z.: Robust aggregation for federated learning. *IEEE Transactions on Signal Processing* **70**, 1142–1154 (2022) <https://doi.org/10.1109/TSP.2022.3153135>
- [18] Jeong, H., Son, H., Lee, S., Hyun, J., Chung, T.-M.: Fedcc: Robust federated learning against model poisoning attacks. *arXiv preprint arXiv:2212.01976* (2022)
- [19] Wang, N., Xiao, Y., Chen, Y., Hu, Y., Lou, W., Hou, Y.T.: Flare: defending federated learning against model poisoning attacks via latent space representations. In: *Proceedings of the 2022 ACM on Asia Conference on Computer and Communications Security*, pp. 946–958 (2022)
- [20] Luong, T.D., Tien, V.M., Quyen, N.H., Hien, D.T.T., Duy, P.T., Pham, V.-H.: Fed-lsae: Thwarting poisoning attacks against federated cyber threat detection system via autoencoder-based latent space inspection. *Journal of Information Security and Applications* **87**, 103916 (2024)
- [21] Melis, L., Song, C., De Cristofaro, E., Shmatikov, V.: Exploiting unintended feature leakage in collaborative learning. In: *2019 IEEE Symposium on Security and Privacy (SP)*, pp. 691–706 (2019). <https://doi.org/10.1109/SP.2019.00029>
- [22] Phong, L.T., Aono, Y., Hayashi, T., Wang, L., Moriai, S.: Privacy-preserving deep learning via additively homomorphic encryption. *IEEE Transactions on Information Forensics and Security* **13**(5), 1333–1345 (2018) <https://doi.org/10.1109/TIFS.2017.2787987>
- [23] Zhu, L., Liu, Z., Han, S.: Deep leakage from gradients. In: Wallach, H., Larochelle, H., Beygelzimer, A., Alché-Buc, F., Fox, E., Garnett, R. (eds.) *Advances in Neural Information Processing Systems*, vol. 32. Curran Associates, Inc., ??? (2019)
- [24] Ma, Z., Ma, J., Miao, Y., Li, Y., Deng, R.H.: Shieldfl: Mitigating model poisoning attacks in privacy-preserving federated learning. *IEEE Transactions on Information Forensics and Security* **17**, 1639–1654 (2022) <https://doi.org/10.1109/TIFS.2022.3169918>
- [25] Liu, H., Zhang, S., Zhang, P., Zhou, X., Shao, X., Pu, G., Zhang, Y.: Blockchain

- and federated learning for collaborative intrusion detection in vehicular edge computing. *IEEE Transactions on Vehicular Technology* **70**(6), 6073–6084 (2021) <https://doi.org/10.1109/TVT.2021.3076780>
- [26] Rathore, S., Park, J.H.: A blockchain-based deep learning approach for cyber security in next generation industrial cyber-physical systems. *IEEE Transactions on Industrial Informatics* **17**(8), 5522–5532 (2021) <https://doi.org/10.1109/TII.2020.3040968>
- [27] Shi, Z., Yang, Z., Hassan, A., Li, F., Ding, X.: A privacy preserving federated learning scheme using homomorphic encryption and secret sharing. *Telecommunication Systems* **82**(3), 419–433 (2023)
- [28] Sahinbas, K., Catak, F.O.: Secure multi-party computation-based privacy-preserving data analysis in healthcare iot systems. In: *Interpretable Cognitive Internet of Things for Healthcare*, pp. 57–72. Springer, ??? (2023)
- [29] Mohassel, P., Zhang, Y.: Secureml: A system for scalable privacy-preserving machine learning. In: *2017 IEEE Symposium on Security and Privacy (SP)*, pp. 19–38 (2017). IEEE
- [30] Liu, F.: Generalized gaussian mechanism for differential privacy. *IEEE Transactions on Knowledge and Data Engineering* **31**(4), 747–756 (2018)
- [31] Cheu, A., Smith, A., Ullman, J., Zeber, D., Zhilyaev, M.: Distributed differential privacy via shuffling. In: Ishai, Y., Rijmen, V. (eds.) *Advances in Cryptology – EUROCRYPT 2019*, pp. 375–403. Springer, Cham (2019)
- [32] Zhang, J., Chen, J., Wu, D., Chen, B., Yu, S.: Poisoning attack in federated learning using generative adversarial nets. In: *2019 18th IEEE International Conference On Trust, Security And Privacy In Computing And Communications/13th IEEE International Conference On Big Data Science And Engineering (TrustCom/Big-DataSE)*, pp. 374–380 (2019). <https://doi.org/10.1109/TrustCom/BigDataSE.2019.00057>
- [33] Zhang, J., Chen, B., Cheng, X., Binh, H.T.T., Yu, S.: Poisongan: Generative poisoning attacks against federated learning in edge computing systems. *IEEE Internet of Things Journal* **8**(5), 3310–3322 (2021) <https://doi.org/10.1109/JIOT.2020.3023126>
- [34] Xie, Y., Fang, M., Gong, N.Z.: *Model Poisoning Attacks to Federated Learning via Multi-Round Consistency* (2024)
- [35] Rodríguez-Barroso, N., Jiménez-López, D., Luzón, M.V., Herrera, F., Martínez-Cámara, E.: Survey on federated learning threats: Concepts, taxonomy on attacks and defences, experimental study and challenges. *Information Fusion* **90**, 148–173 (2023) <https://doi.org/10.1016/j.inffus.2022.09.011>

- [36] Lin, Z., Shi, Y., Xue, Z.: Idsgan: Generative adversarial networks for attack generation against intrusion detection, 79–91 (2022) https://doi.org/10.1007/978-3-031-05981-0_7
- [37] Kornblith, S., Norouzi, M., Lee, H., Hinton, G.: Similarity of Neural Network Representations Revisited (2019)
- [38] Son, H.M., Kim, M.H., Chung, T.-M.: Comparisons where it matters: Using layer-wise regularization to improve federated learning on heterogeneous data. *Applied Sciences* **12**(19), 9943 (2022)
- [39] Ferrag, M.A., Friha, O., Hamouda, D., Maglaras, L., Janicke, H.: Edge-IIoTset: A New Comprehensive Realistic Cyber Security Dataset of IoT and IIoT Applications: Centralized and Federated Learning. <https://doi.org/10.21227/mbc1-1h68>
- [40] Sharafaldin, I., Lashkari, A.H., Ghorbani, A.A., *et al.*: Toward generating a new intrusion detection dataset and intrusion traffic characterization. *ICISSp* **1**, 108–116 (2018)